Research Square

Preprints are preliminary reports that have not undergone peer review.
They should not be considered conclusive, used to inform clinical practice,
or referenced by the media as validated information.

Selective uranium capture from nitric acid media using a PS-GMA-supported phenanthroline diamide sorbent

Tianpei Cai
Yancheng Institute of Technology
Hengye Li
Yancheng Institute of Technology
Juanjuan Gao
Yancheng Institute of Technology
Han Wu
Dalian Institute of Chemical Physics
Xiaolong He
Dalian Institute of Chemical Physics
Xiaoyu Sun
1260456900@qq.com
Yancheng Institute of Technology
Wei Wang
Yancheng Institute of Technology

Research Article

Keywords: Solid-phase extraction, Chelating resin, Uranium adsorption, 1,10-Phenanthroline ligand, Nitric acid, Competitive adsorption

Posted Date: November 9th, 2026

DOI: https://doi.org/10.21203/rs.3.rs-11347103/v1

License: This work is licensed under a Creative Commons Attribution 4.0 International License.
Read Full License

Additional Declarations: No competing interests reported.

Selective uranium capture from nitric acid media using a PS-GMA-supported phenanthroline diamide sorbent

Tianpei Cai[1], Hengye Li[1], Juanjuan Gao[1], Han Wu[2], Xiaolong He[2], Xiaoyu Sun[1,*], Wei Wang[1,*]

[1] *School of Chemistry and Chemical Engineering, Yancheng Institute of Technology, Yancheng 224002, PR China*

[2] *Dalian Institute of Chemical Physics, Chinese Academy of Sciences, Dalian 116023, China*

E-mail addresses: caitianpei@ycit.edu.cn; lhy1024006@sina.com; gaojj@ycit.edu.cn; hanwu89@dicp.ac.cn; jx_hexl@dicp.ac.cn

* Corresponding authors: Xiaoyu Sun (1260456900@qq.com); Wei Wang (wangw@ycit.edu.cn).

Abstract

A phenanthroline diamide ligand was immobilized on glycidyl methacrylate-modified polystyrene for uranium adsorption from nitric acid. Increasing acidity enhanced discrimination against rare-earth ions. Columns retained over 99.7% of uranium from dilute single-component solutions and 79.07% in a multicomponent sample containing a combined 2500-fold excess of ten metal ions. Competitive batch tests showed appreciable Fe and Ru co-uptake. The lowest column effluent concentration was 0.0563 μg L^{-1}. Small-volume simulated digestion tests gave 96.60–98.85% apparent retention, corresponding to 64.40–65.90 mg g^{-1} under the tested conditions. The material shows potential for selective uranium retention in nitric acid media.

Article Highlights

- Phenanthroline diamide was attached to polymer microspheres to study uranium capture.
- Higher nitric acid concentration improves uranium discrimination against rare-earth ions.
- Column effluent uranium reached 0.0563 μg L^{-1} (0.0563 ppb) under the tested conditions.

Keywords

Solid-phase extraction; Chelating resin; Uranium adsorption; 1,10-Phenanthroline ligand; Nitric acid; Competitive adsorption

1. Introduction

The separation of uranium from lanthanide elements is relevant to nuclear and rare-earth processing. Nitric-acid solutions containing uranium and other metals provide a demanding medium for evaluating selective sorbents. Solvent extraction has been extensively investigated for actinide separation, including the use of diglycolamide and nitrogen-donor ligands [1, 2, 3]. Solid sorbents offer a complementary route for studying selective uranium capture, but their suitability for a particular process depends on loading capacity, achievable throughput, and recovery of the retained uranium.

Solid-phase extraction (SPE) and extraction chromatography based on functionalized resins have been developed for metal separation and preconcentration [4, 5]. Immobilizing a chelating ligand on a polymer support provides a route to combining ligand selectivity with column operation. Glycidyl methacrylate-based chelating resins have been examined for uranium removal from aqueous solutions [6], and functionalized poly(glycidyl methacrylate) materials have coupled uranium adsorption with desorption and reuse studies [7]. Diamide-functionalized polymer spheres bearing malonamide or diglycolamide groups

have also been examined for uranyl adsorption from dilute solutions of low acidity [8]. Extraction chromatography with a diglycolamic-acid-coated polymeric resin has been investigated for low-concentration uranium-bearing feeds [9]. In radioanalytical sample preparation, uranium isolation with UTEVA resin can be coupled with controlled elution before mass-spectrometric measurement [10]. These findings motivate examination of how ligand structure and nitric acid concentration affect uranium uptake in polymer-supported systems.

Among candidate chelating groups, 1,10-phenanthroline derivatives are especially attractive because their nitrogen donor sites offer strong actinide affinity and actinide/lanthanide discrimination in acidic media [11, 12]. In solution, phenanthroline-derived pyrrolidone ligands have been used for uranium separation [13], while 2,9-diamide-1,10-phenanthroline ligands have enabled U(VI)/Mo(VI) [14] and U(VI)/Pu(IV) separations at high acidity [15]. The same coordination motif has been transferred to heterogeneous sorbents by anchoring phenanthroline ligands onto hierarchically mesoporous silica [16], carbon-doped boron nitride [17], or graphene oxide [18].

These prior studies mainly address soluble phenanthroline extractants or inorganic porous supports. Here, we prepared 2,9-bis(N-(1-imidazolyl)propylaminocarbonyl)-1,10-phenanthroline (IAP) and reacted it with PS-GMA according to the designed functionalization procedure; the resulting material is denoted PS-IAP. This study examines time-dependent uranium uptake, acidity-dependent U/rare-earth element (REE) discrimination, adsorption after acid exposure, and retention in multicomponent solutions, including a simulated spent-fuel digestion matrix. Its contribution is the evaluation of an imidazolyl-substituted phenanthroline diamide on a PS-GMA support across these laboratory tests. The objective is to assess the material's uranium-retention behavior and potential in nitric acid media. Bulk uranium recovery from spent-fuel solutions is not demonstrated by the present experiments.

2. Experimental

2.1 Materials

2,9-Dimethyl-1,10-phenanthroline, selenium dioxide, 4-bromobutylamine hydrobromide, 1-(3-aminopropyl)imidazole, N,N′-carbonyldiimidazole (CDI), and N,N-diisopropylethylamine (DIPEA) were purchased from Shanghai Aladdin Biochemical Technology Co., Ltd. (Shanghai, China). Acetonitrile, ethanol, cyclohexane, N,N-dimethylformamide (DMF), and sodium carbonate were obtained from Shanghai Titan Technology Co., Ltd. (Shanghai, China). Acetone and diethyl ether were purchased from Xilong Scientific Co., Ltd. (Chengdu, China). All reagents above were of analytical grade and used without further purification. Chromatographic-grade methanol was purchased from Sigma-Aldrich (Shanghai, China). Glycidyl methacrylate-modified polystyrene microspheres (PS-GMA) were provided by Dalian Institute of Chemical Physics, Chinese Academy of Sciences.

2.2 Characterization

Metal-ion concentrations were determined by inductively coupled plasma mass spectrometry (ICP-MS; Agilent 7700, Beijing, China) or inductively coupled plasma optical emission spectrometry (ICP-OES), as specified below. The precursor and IAP were characterized by electrospray ionization mass spectrometry (ESI-MS) in negative-ion mode. Column loading was performed with a syringe pump (TYD02-01-CE, China). A magnetic stirrer (RCT basic) and a rotary evaporator (RV3) were purchased from IKA (Guangzhou) Instrument Co., Ltd. A mechanical stirrer (S-90C) was obtained from Shanghai Shen Sheng Biotechnology Co., Ltd., and a rotary mixer (QB-128) from Haimen Kylin-Bell Laboratory Instruments Co., Ltd. All reported uranium concentrations and adsorption amounts are expressed on an elemental-U mass basis. In the experimental records, ppm and ppb denote mass concentrations (1 ppm = 1 mg L^{-1} and 1 ppb = 1 μg L^{-1}), not mass fractions.

2.3 Preparation of the PS-IAP chelating SPE packing

2.3.1 Synthesis of 1,10-phenanthroline-2,9-dicarboxylic acid

Selenium dioxide (5.62 g, 50 mmol) was added to a mixture of 1,4-dioxane (150 mL) and water (10 mL), and the mixture was heated to reflux. A solution of 2,9-dimethyl-1,10-phenanthroline (5.02 g, 24 mmol) in 100 mL of 1,4-dioxane was then added dropwise over 10 min, and the reaction was continued under reflux for 1 h. The hot solution was filtered immediately, and the filtrate was cooled to room temperature to give yellow needle-like crystals. The crystals were collected by filtration and washed with warm dioxane. The crystals were dissolved in 85 mL of concentrated nitric acid and refluxed with stirring for 2 h. The reaction mixture was cooled and poured into 30 g of ice, and the mixture was allowed to stand until a precipitate appeared. The precipitate was collected by filtration and washed with water and diethyl ether, yielding a pale yellow solid powder. The obtained 1,10-phenanthroline-2,9-dicarboxylic acid was used directly in the next step without further purification.

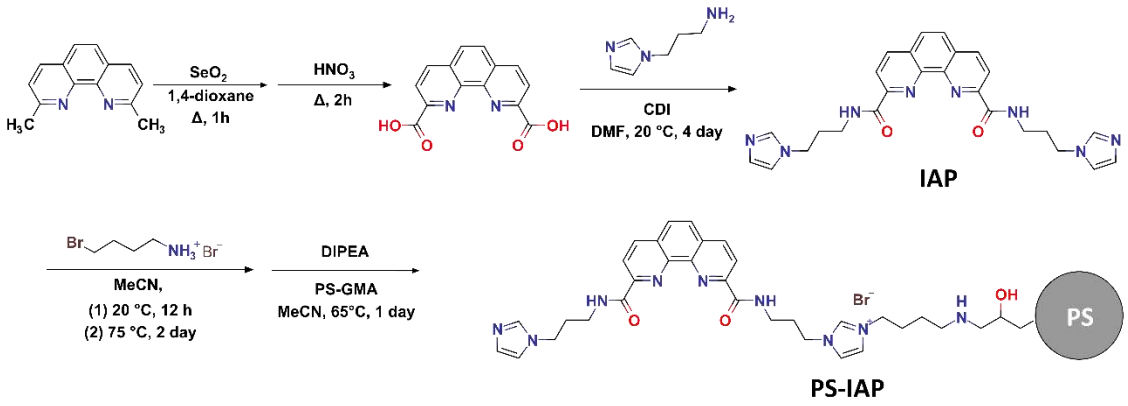
2.3.2 Synthesis of IAP

The 1,10-phenanthroline-2,9-dicarboxylic acid (4.5 g, 16.8 mmol) obtained above was dissolved in 95 mL of DMF, and the solution was heated to 45 °C. CDI (8.55 g, 52.73 mmol) was then added in portions, and the reaction was continued at 45 °C for 2 h. Subsequently, 4.30 mL (36.0 mmol) of 1-(3-aminopropyl)imidazole was added dropwise at 20 °C, and the mixture was stirred at room temperature for 4 days. After the reaction was complete, an appropriate amount of water was added and the mixture was distilled under reduced pressure to remove DMF. The residue was mixed with 200 mL of Na_2CO_3 solution (1 mol L^{-1}) and kept at 5 °C overnight. The resulting precipitate was collected, washed successively with water and diethyl ether, and dissolved in a mixture of acetonitrile and ethanol. The turbid yellow solution was filtered to remove insoluble material, giving a clear yellow solution. The solvent was removed by rotary evaporation, producing a brown liquid that solidified into a yellowish-white solid after standing at 60 °C overnight; this

127 solid was the target ligand 2,9-bis(N-(1-imidazolyl)propylaminocarbonyl)-1,10-
128 phenanthroline (IAP).

129 *2.3.3 Preparation of PS-IAP*

130 4-Bromobutylamine hydrobromide (2.34 g, 10.05 mmol) was dissolved in 10 mL of
131 acetonitrile, and the solution was added dropwise to 90 mL of an acetonitrile/ethanol
132 mixture (v:v = 8:1) containing 2.0 g of IAP (4.15 mmol). The mixture was stirred at 20 °C
133 for 12 h and then at 75 °C for 2 days. DIPEA (12 mmol) was added and stirring was
134 continued for 2 h. The solvent was removed under reduced pressure, and the residue was
135 washed with n-hexane and dried in a vacuum oven. The resulting product was dissolved in
136 a mixture of acetonitrile (20 mL) and ethanol (15 mL), and 2.5 g of PS-GMA was dispersed
137 in this solution. The mixture was mechanically stirred at 65 °C for 24 h. The reacted
138 mixture was centrifuged, and the product was washed successively with ethanol, water,
139 and acetone, yielding the PS-IAP chelating SPE packing. The preparation process is
140 illustrated in Fig. 1.



141

142 **Fig. 1** Proposed functionalization route for the preparation of PS-IAP

2.4 Adsorption experiments

2.4.1 Batch adsorption kinetics of U(VI)

PS-IAP (20 mg) was added to 100 mL of 0.1 mol L^{-1} HNO_3 containing 20 mg L^{-1} U(VI). Aliquots were collected after 5, 10, 15, 30, 45, 120, and 360 min, and the residual uranium concentration was measured by ICP-OES. The adsorption amount at time *t* was calculated using $q_t = (C_o - C_t)V/m$, where C_o and C_t are the uranium concentrations initially and at time *t*, respectively; *V* is the solution volume, and *m* is the sorbent mass.

The pseudo-first-order (PFO) and pseudo-second-order (PSO) models [19, 20] were fitted to the seven reported uptake values by nonlinear least squares in the original q_t scale, using Eqs. (1) and (2), respectively:

$$q_t = q_e[1 - exp(-k_1 t)] \quad (1)$$

$$q_t = \frac{k_2 {q_e}^2 t}{1 + k_2 q_e t} \quad (2)$$

Here, q_t and q_e are the uptake at time t and the fitted asymptotic uptake (mg g^{-1}), respectively; k_1 (min^{-1}) and k_2 (g mg^{-1} min^{-1}) are the PFO and PSO rate constants. Both models impose $q_t = 0$ at $t = 0$; no artificial zero-time observation was added. All seven values were retained and assigned equal weights because replicate-level uncertainties were not available for fitting. Positive parameters were estimated using nonlinear least squares in SciPy 1.16.3. Model performance was compared using residuals, the residual sum of squares (SSE), the root-mean-square error (RMSE, calculated as the square root of SSE/n), and R^2 (1 − SSE/SST), where n = 7 and SST is the sum of squared deviations of the observed uptake values from their mean. The models were compared on the same untransformed response scale to avoid biases associated with comparing different linearized forms [19].

2.4.2 Adsorption in nitric acid solutions of different concentrations

Nitric acid solutions (0.005, 0.025, 0.050, 0.250, 0.500, 1.000, and 1.500 mol L^{-1}) were prepared, each containing uranium (47.6 mg L^{-1}) and four REEs (La, 43.6 mg L^{-1}; Sm, 34.2 mg L^{-1}; Yb, 47.9 mg L^{-1}; Y, 22.6 mg L^{-1}). PS-IAP (10 mg) was dispersed in 20 mL of each solution and shaken for 2 h. After standing for 10 min, the supernatant was analyzed by ICP-MS, and the adsorption efficiencies were calculated.

2.4.3 Uranium adsorption after nitric acid exposure

PS-IAP (20 mg) was continuously stirred in 1.0 mol L^{-1} HNO_3 for 2 h, 2.0 mol L^{-1} HNO_3 for 24 h, or 3.0 mol L^{-1} HNO_3 for 72 h. After acid treatment, the sorbent was recovered and continuously stirred with 100 mL of a U(VI) solution containing 10 mg L^{-1} uranium in 1.0 mol L^{-1} HNO_3 for 2 h. The adsorption amount was then determined from the uranium concentrations before and after adsorption.

2.4.4 Measurement of uranium adsorption efficiency during column loading

An SPE column packed with 0.3 g of PS-IAP was prepared. A 20 mL portion of 1 mol L^{-1} HNO_3 containing 0.2 mg L^{-1} uranium was loaded on the column at 0.2, 1.0, or 2.0 mL min^{-1}. The uranium concentration in the effluent was determined by ICP-MS, and the apparent retention percentage was calculated from the difference between the uranium mass loaded and that measured in the effluent. This solution-based calculation estimates apparent retention; uranium on the sorbent was not independently quantified.

2.4.5 Effect of coexisting metal ions on uranium adsorption by PS-IAP

A mixed solution containing Fe^{3+}, Zn^{2+}, Ni^{2+}, Co^{2+}, Cu^{2+}, Zr^{4+}, Pb^{2+}, Cs^{+}, Ba^{2+}, Ru^{3+}, and UO_2^{2+} was prepared in 1.5 mol L^{-1} HNO_3. The concentration of each of the ten coexisting metal ions was 50 mg L^{-1}, and the uranium concentration was 0.2 mg L^{-1}. A 100 mL portion

of this solution was loaded at 2.0 mL min^{-1} onto an SPE column packed with 0.3 g of PS-IAP. The uranium concentration in the loading effluent was measured to evaluate the effect of the coexisting metal ions on uranium adsorption by PS-IAP.

2.4.6 Competitive adsorption of uranium and ten coexisting metal ions under acidic conditions

A 100 mL mixed solution containing UO_2^{2+} and ten coexisting metal ions (Fe^{3+}, Zn^{2+}, Ni^{2+}, Co^{2+}, Cu^{2+}, Zr^{4+}, Pb^{2+}, Cs^{+}, Ba^{2+}, and Ru^{3+}) was prepared in 1.5 mol L^{-1} HNO_3, with each of the eleven metal ions at 20 mg L^{-1}. PS-IAP (40 mg) was then added, and the suspension was stirred at room temperature for 12 h. The concentrations of all eleven metal ions before and after adsorption were determined by ICP-MS.

2.4.7 Adsorption from simulated spent-fuel digestion solution

Two tests were performed using loading solutions containing 1.0 or 2.0 mol L^{-1} HNO_3. An SPE cartridge was packed with 0.3 g of PS-IAP, washed with 10 mL of deionized water, and conditioned with nitric acid at the concentration used for loading. In each test, 0.2 mL of simulated digestion solution (Table 1) was loaded, followed by a 10 mL rinse with HNO_3 of the same concentration. The combined effluent was collected for determination of its uranium content. The reported retention percentage was calculated as 100 × (uranium mass loaded − uranium mass in the combined effluent)/(uranium mass loaded). The nitric acid rinse was part of the loading and washing sequence; no separate elution step was evaluated.

Table 1 Elemental composition of the simulated spent-fuel digestion solution

Elements	Concentration (mg L^{-1})	Elements	Concentration (mg L^{-1})
Y	167.22	Eu	51.27
La	447.39	Gd	29.80
Ce	872.65	Tb	0.76

Elements	Concentration (mg L^{-1})	Elements	Concentration (mg L^{-1})
Pr	411.83	Dy	0.35
Nd	1482.55	Zr	1315
Sm	291.17	U	100000.00

3. Results and discussion

3.1 Preparation and ESI-MS mass-spectrometric characterization of IAP ligand

The synthesis of IAP and the functionalization procedure used to prepare PS-IAP are summarized in Fig. 1. In the negative-ion ESI-MS spectra, 1,10-phenanthroline-2,9-dicarboxylic acid gave an $[M-H]^-$ ion at m/z 267.0414, whereas the IAP ligand gave a new $[M-H]^-$ ion at m/z 481.2105 (calculated 481.2106). The observed mass increase is consistent with the conversion of the two carboxylic acid groups into the corresponding amide substituents and with the expected molecular mass of the IAP ligand (Figs. S1 and S2).

3.2 Batch adsorption kinetics and column-loading performance

Batch adsorption kinetics were first examined to follow the time dependence of uranium uptake. Adsorption increased from 1.591 mg g^{-1} at 5 min to 15.27 mg g^{-1} at 45 min, followed by a smaller increase to 15.88 mg g^{-1} at 360 min (Fig. 2). Nonlinear fitting gave a closer description with the PFO model (R^2 = 0.9357; RMSE = 1.294 mg g^{-1}) than with the PSO model (R^2 = 0.8775; RMSE = 1.786 mg g^{-1}). The PFO parameters were q_e = 16.11 mg g^{-1} and k_1 = 0.05817 min^{-1}, whereas the PSO parameters were q_e = 17.92 mg g^{-1} and k_2 = 0.004056 g mg^{-1} min^{-1} (Table 2). The PFO asymptote was closer to the final measured uptake. These fitted q_e values describe the present kinetic experiment and are not saturation capacities derived from an adsorption isotherm.

Table 2 Nonlinear kinetic model parameters for uranium uptake on PS-IAP

Model	q_e (mg g^{-1})	Rate constant	SSE (mg^2 g^{-2})	RMSE (mg g^{-1})	R^2
PFO	16.11	k_1 = 0.05817 min^{-1}	11.720	1.294	0.9357
PSO	17.92	k_2 = 0.004056 g mg^{-1} min^{-1}	22.335	1.786	0.8775

All seven time points were fitted with equal weights and two positive free parameters per model. RMSE = √(SSE/7). q_e is the fitted asymptotic uptake under the kinetic-test conditions, not an isotherm-derived saturation capacity.

As seen in Fig. 2 and Table 2, the PFO model provided a better fit to the experimental data than the PSO model, with a higher R^2 and a lower RMSE. The equilibrium adsorption capacity estimated by the PFO model (16.11 mg g^{-1}) was close to the measured uptake at 360 min (15.88 mg g^{-1}). These results indicate that the PFO model adequately describes the uranium adsorption kinetics of PS-IAP under the investigated conditions.

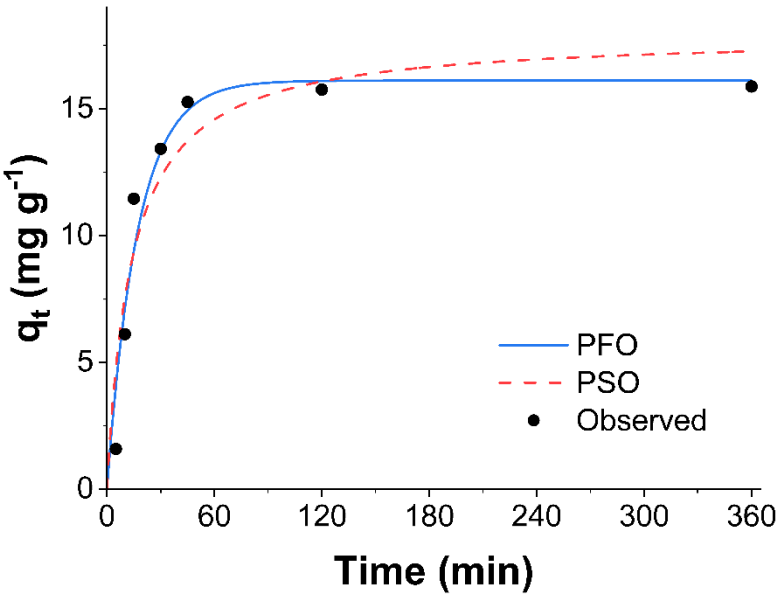


Fig. 2 Nonlinear PFO and PSO fits to uranium uptake on PS-IAP. Symbols represent the seven reported observations; lines are model predictions. Conditions: HNO_3 = 0.1 mol L^{-1}; $C_0(U)$ = 20 mg L^{-1}; solution volume = 100 mL; PS-IAP = 20 mg

For 20 mL samples loaded onto columns containing 0.3 g of PS-IAP, apparent uranium retention exceeded 99.7% at loading flow rates of 0.2–2.0 mL min^{-1} (Table 3). At 2.0 mL min^{-1}, the uranium concentration decreased from 195.8 μg L^{-1} in the loading solution to 0.0563 μg L^{-1} in the effluent, corresponding to 99.97% apparent retention. These results demonstrate effective uranium retention from dilute nitric acid solutions under the tested column-loading conditions. Dynamic saturation capacity and breakthrough volume were not determined in these experiments.

Table 3 Apparent uranium retention by PS-IAP at different loading flow rates

Loading flow rate (mL min^{-1})	Uranium concentration in loading solution (μg L^{-1})	Loading amount (ng)	Uranium concentration in effluent (μg L^{-1})	Content in effluent (ng)	Apparent retention (%)
0.2	195.8	3916	0.1025	2.050	99.95
1	164.0	3280	0.4800	9.600	99.71
2	195.8	3916	0.0563	1.126	99.97

3.3 Acidity-dependent U/REE adsorption and uptake after acid exposure

Solution acidity can influence both metal-ion speciation and ligand protonation. Increasing the HNO_3 concentration produced opposite adsorption trends for uranium and the four REEs (Fig. 3). At 1.5 mol L^{-1} HNO_3, uranium adsorption approached 90%, whereas adsorption of Y, La, Sm, and Yb did not exceed approximately 13%. These results show acidity-dependent U/REE discrimination within the tested composition and contact time.

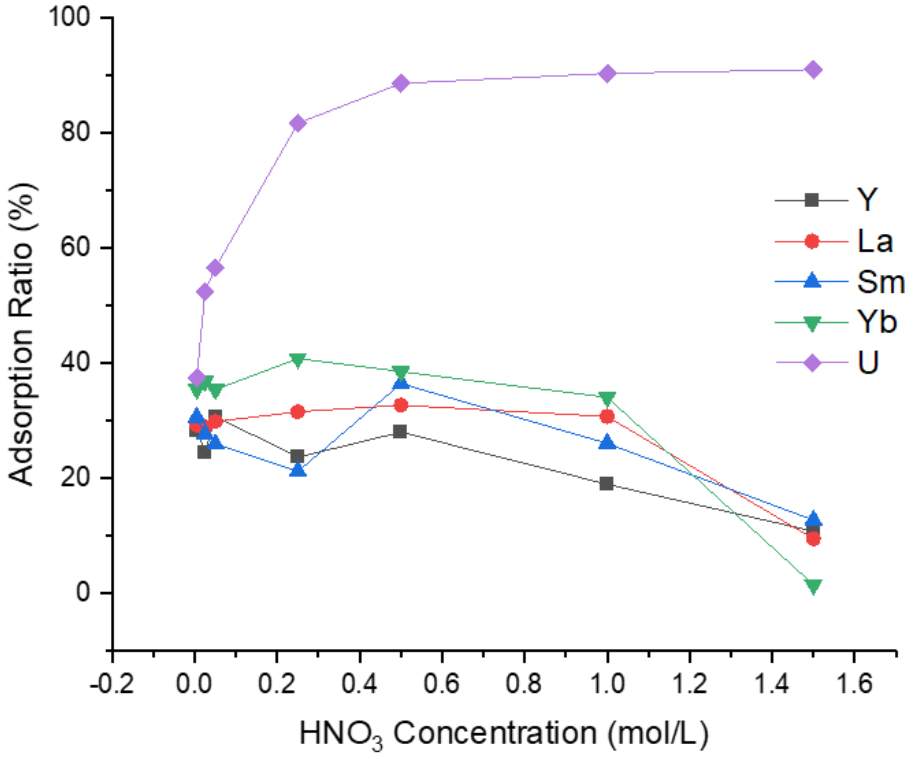


Fig. 3 Adsorption efficiencies of PS-IAP for uranium and four rare-earth elements at different nitric acid concentrations. Conditions: U = 47.6 mg L^{-1}; La = 43.6 mg L^{-1}; Sm = 34.2 mg L^{-1}; Yb = 47.9 mg L^{-1}; Y = 22.6 mg L^{-1}; solution volume = 20 mL; PS-IAP = 10 mg; contact time = 2 h

The acidity-dependent uranium uptake by PS-IAP may reflect the combined effects of uranyl–ligand coordination, nitrate association, and protonation of ligand donor sites. Related phenanthroline diamide ligands form 1:1 uranyl complexes in solution [14, 15], while a DAPhen-functionalized carbon-doped boron nitride sorbent exhibits uranium/lanthanide selectivity in nitric acid [17]. These findings are consistent with a possible contribution of ligand coordination to uranium retention by PS-IAP, although the binding geometry and stoichiometry on the immobilized sorbent remain undetermined. Because H^+ and nitrate concentrations varied together here, their separate contributions cannot be resolved. Direct coordination measurements would be required to distinguish these effects from changes in sorbent-site accessibility which may be studied in our future work.

Uranium uptake was also measured after nitric acid exposure. After treatment in 1.0 mol L^{-1} HNO_3 for 2 h, 2.0 mol L^{-1} HNO_3 for 24 h, or 3.0 mol L^{-1} HNO_3 for 72 h, PS-IAP gave adsorption amounts of 12.05–13.03 mg g^{-1} in the subsequent uptake tests using 20 mg of sorbent and an initial uranium concentration of 10 mg L^{-1} (Table 4). Uptake therefore remained measurable after each exposure. Acid concentration and exposure time were varied together, and a matched untreated reference and ligand-leaching measurements were not reported. These results cannot quantify capacity retention or establish long-term structural stability.

Table 4 Uranium adsorption amount of PS-IAP after nitric-acid treatment

HNO_3 concentration (mol L^{-1})	**Acid treatment time (h)**	**U adsorption amount (mg g^{-1})**
1.0	2	12.05
2.0	24	12.42
3.0	72	13.03

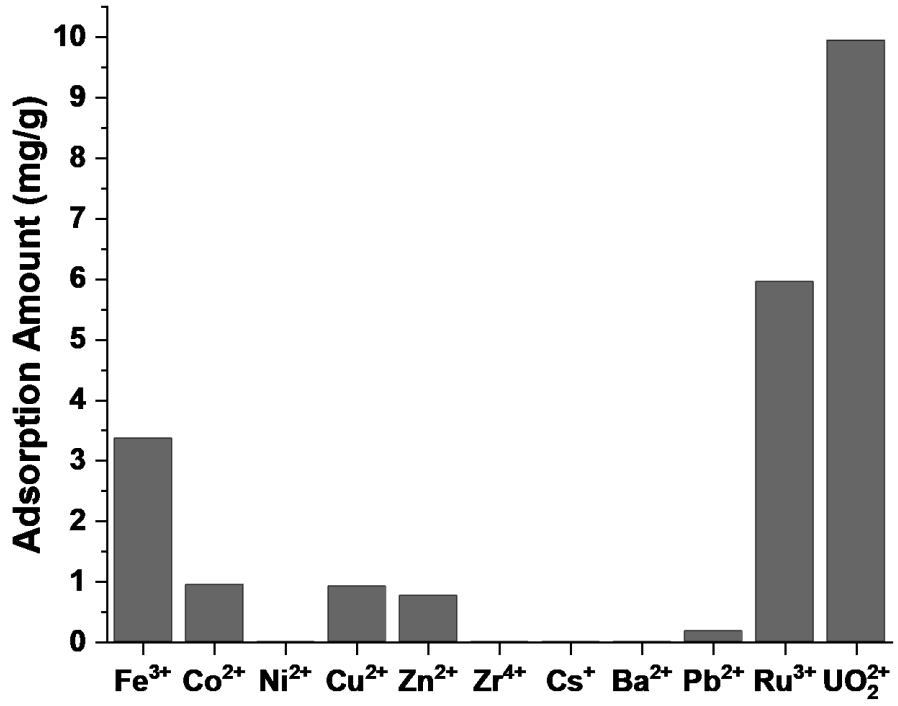
3.4 Selectivity in the presence of coexisting metal ions

To determine whether abundant coexisting metal ions suppress uranium capture during column operation, a mixed solution containing ten coexisting metal ions at a combined concentration 2500 times that of uranium was loaded onto the PS-IAP column. Compared with the uranium adsorption efficiency of 99.97% obtained from the uranium-only solution at the same loading flow rate (Table 3), the adsorption efficiency decreased to 79.07% in the multicomponent solution. Nevertheless, PS-IAP reduced the uranium concentration from 190.65 to 39.895 μg L^{-1}, corresponding to a residual concentration below 40 μg L^{-1} (Table 5). These results demonstrate that even with measurable interference from the coexisting metal ions, PS-IAP still retained substantial uranium-capture capability under a severe excess of competing ions.

Table 5 Uranium retention by PS-IAP in the presence of ten coexisting metal ions

Loading volume (mL)	Uranium concentration in loading solution (μg L^{-1})	Uranium concentration in effluent (μg L^{-1})	Apparent retention (%)
100	190.65	39.895	79.07

To identify the principal interfering species, competitive batch adsorption of UO_2^{2+} and ten coexisting metal ions was performed in 1.5 mol L^{-1} HNO_3, with all eleven ions initially present at 20 mg L^{-1}. As shown in Fig. 4, PS-IAP exhibited negligible adsorption of Cs^+, Ba^{2+}, Ni^{2+}, and Zr^{4+} and only weak adsorption of Co^{2+}, Cu^{2+}, Zn^{2+}, and Pb^{2+}. In contrast, appreciable adsorption was observed for Fe^{3+} and Ru^{3+}, suggesting that these ions can compete more effectively for the chelating sites of PS-IAP. Despite the presence of multiple competing ions, UO_2^{2+} exhibited the highest adsorption amount of 9.95 mg g^{-1}, showing preferential affinity of PS-IAP for uranium under the tested acidic conditions. The appreciable co-uptake of Fe^{3+} and Ru^{3+} suggests that these ions are potential competitors for uranium adsorption under the tested conditions.



304

305 **Fig. 4** Competitive adsorption of UO_2^{2+} and ten coexisting metal ions by PS-IAP under
306 acidic conditions. Conditions: HNO_3 concentration = 1.5 mol L^{-1}; 20 mg L^{-1} of each ion;
307 solution volume = 100 mL; PS-IAP = 40 mg; contact time = 12 h

308 ## 3.5 Uranium adsorption from simulated spent-fuel digestion solution

309 PS-IAP was tested with the simulated spent-fuel digestion composition listed in Table 1.
310 Each experiment loaded 0.2 mL of solution containing 20 mg uranium onto 0.3 g of
311 sorbent. Uranium in the combined loading effluent and acid rinse was 0.68 mg at 1.0 mol
312 L^{-1} HNO_3 and 0.23 mg at 2.0 mol L^{-1} HNO_3. The corresponding apparent retention
313 percentages were 96.60% and 98.85% (Table 6), equivalent to retained amounts of 19.32
314 and 19.77 mg and conditional loadings of 64.40 and 65.90 mg g^{-1}. These values are inferred
315 from the solution measurements; they are not independently measured sorbent uranium
316 contents or recovered-product yields.

Table 6 Apparent uranium retention by PS-IAP from simulated spent-fuel digestion solution

	Sample A	Sample B
Nitric acid concentration in loading solutions (mol L^{-1})	1.0	2.0
Uranium content in the simulated spent-fuel loading solution (mg)	20	20
Uranium content in the effluent (mg)	0.68	0.23
Apparent retention (%)	96.60	98.85

Besides, the simulated matrix represents only the listed elements and nitric acid concentrations. It does not reproduce the full composition or radiation environment of an actual spent-fuel solution. The results support uranium retention in this defined multicomponent test, while applicability to real processing solutions still requires separate validation.

4. Conclusions

PS-IAP was prepared using the IAP ligand and PS-GMA microspheres, with negative-ion ESI-MS supporting the formation of the free ligand. Batch uranium uptake reached 15.27 mg g^{-1} at 45 min and 15.88 mg g^{-1} at 360 min. The PFO model described the uranium uptake profile more closely than the PSO model under the investigated conditions. Increasing nitric acid concentration enhanced U/REE discrimination, and uranium uptake was observed after the specified acid exposures. Columns containing 0.3 g PS-IAP retained more than 99.7% of uranium from 20 mL uranium-only samples and 79.07% from a 100 mL multicomponent sample. The lowest measured uranium concentration in the column effluent was 0.0563 μg L^{-1}. Competitive batch tests showed appreciable Fe and Ru co-uptake. For 0.2 mL simulated digestion samples containing 20 mg uranium, apparent retention reached 96.60–98.85%, corresponding to conditional loadings of 64.40–65.90 mg g^{-1}.

The uranium uptake and acidity-dependent U/REE discrimination observed under the tested conditions suggest that PS-IAP has potential as a sorbent for selective uranium retention in nitric acid media. Its process applicability remains to be evaluated through adsorption isotherms, breakthrough measurements, elution, and regeneration studies. The present results do not establish the feasibility of bulk uranium recovery from spent-fuel solutions.

Declarations

Author contributions statement

Tianpei Cai, Xiaoyu Sun and Wei Wang conceived the study. Tianpei Cai developed the experimental methods with Han Wu and Xiaolong He. Tianpei Cai, Hengye Li and Juanjuan Gao performed the experiments and curated the data. Tianpei Cai analyzed the data and prepared the figures. Hengye Li, Juanjuan Gao, Han Wu and Xiaolong He validated the results. Han Wu and Xiaolong He provided resources. Tianpei Cai, Hengye Li and Wei Wang acquired funding. Xiaoyu Sun and Wei Wang supervised the research and managed the project. Tianpei Cai wrote the first draft. Han Wu, Xiaoyu Sun and Wei Wang reviewed and edited the manuscript. All authors approved the final manuscript and accept responsibility for the accuracy and integrity of the work.

Declaration of competing interest

The authors declare that they have no known competing financial interests or personal relationships that could have appeared to influence the work reported in this paper.

Acknowledgements

This work was supported by the National Natural Science Foundation of China (Grant Nos. 22304151, 21974120 and 22176166).

Data availability

Data will be made available on request.

Declaration of generative AI and AI-assisted technologies in the manuscript preparation process

During the preparation of this work, the authors used OpenAI Codex to improve language, readability, manuscript organization, and formatting. After using this tool, the authors reviewed and edited the content as needed and take full responsibility for the content of the published article.

Supplementary information

The supplementary information contains negative-ion electrospray ionization mass spectra of the precursor and the free ligand (Figs. S1 and S2).

References

1. Ansari SA, Pathak P, Mohapatra PK, Manchanda VK (2012) Chemistry of Diglycolamides: Promising Extractants for Actinide Partitioning. Chem Rev 112:1751–1772. https://doi.org/10.1021/cr200002f
2. Ekberg C, Fermvik A, Retegan T, Skarnemark G, Foreman MRS, Hudson MJ, Englund S, Nilsson M (2008) An overview and historical look back at the solvent extraction using nitrogen donor ligands to extract and separate An(III) from Ln(III). Radiochim Acta 96:225–233. https://doi.org/10.1524/ract.2008.1483
3. Kolarik Z, Müllich U, Gassner F (1999) Selective extraction of Am(III) over Eu(III) by 2,6-ditriazolyl- and 2,6-ditriazinylpyridines. Solvent Extr Ion Exch 17:23–32. https://doi.org/10.1080/07360299908934598
4. Horwitz EP, Dietz ML, Chiarizia R, Diamond H, Essling AM, Graczyk D (1992) Separation and preconcentration of uranium from acidic media by extraction

chromatography. Anal Chim Acta 266:25–37. https://doi.org/10.1016/0003-2670(92)85276-C

5. Płotka-Wasylka J, Szczepańska N, de la Guardia M, Namieśnik J (2016) Modern trends in solid phase extraction: New sorbent media. TrAC Trends Anal Chem 77:23–43. https://doi.org/10.1016/j.trac.2015.10.010

6. Donia AM, Atia AA, Moussa EMM, El-Sherif AM, Abd El-Magied MO (2009) Removal of uranium(VI) from aqueous solutions using glycidyl methacrylate chelating resins. Hydrometallurgy 95:183–189. https://doi.org/10.1016/j.hydromet.2008.05.037

7. Tolba AA, Gwad EA, Rashad MM, Shalaby ZM, Kassab WA, Kawady NA, Mohammady SE, Orabi AH (2026) Functionalized poly(glycidylmethacrylate) for selective uranium(VI) adsorption: experimental and theoretical calculation insights. RSC Adv 16:6747–6767. https://doi.org/10.1039/D5RA08591H

8. Peng X, Liu X, Cui Y, Li Y, Ma J, Sun G (2021) Adsorption of uranyl ion with polymer spheres modified by diamide. J Radioanal Nucl Chem 327:395–402. https://doi.org/10.1007/s10967-020-07506-w

9. Selvan BR, Suneesh AS, Ramanathan N (2023) Diglycolamic acid coated cation exchange adsorbent for uranium removal by extraction chromatography. J Radioanal Nucl Chem 332:1775–1786. https://doi.org/10.1007/s10967-023-08869-6

10. Wood AD, Dunn SA, Kaye P, Higginson M, Robb J, Harrison RW (2026) Sample preparation for actinide isotopic analysis using FIB-SEM. J Radioanal Nucl Chem 335:2415–2424. https://doi.org/10.1007/s10967-025-10667-1

11. Lewis FW, Harwood LM, Hudson MJ, Drew MGB, Desreux JF, Vidick G, Bouslimani N, Modolo G, Wilden A, Sypula M, Vu TH, Simonin JP (2011) Highly Efficient Separation of Actinides from Lanthanides by a Phenanthroline-Derived Bis-triazine Ligand. J Am Chem Soc 133:13093–13102. https://doi.org/10.1021/ja203378m

12. Nash KL (1993) A review of the basic chemistry and recent developments in trivalent f-elements separations. Solvent Extr Ion Exch 11:729–768. https://doi.org/10.1080/07366299308918184

13. Wang Y, Hu B, Li Q, Wu Y, Shang X, Yang P, Cai Y, Yuan L, Feng W (2022) Novel phenanthroline-derived pyrrolidone ligands for efficient uranium separation: Liquid-liquid extraction, spectroscopy, and molecular simulations. J Mol Liq 364:119909. https://doi.org/10.1016/j.molliq.2022.119909
14. Xiu TY, Zhang S, Ren P, Liu S, Wang S, Shehzad H, Wang J, Zhang M, Ye G, Jiao C, Wu Q, Yuan L, Chai Z, Shi W (2023) Efficacious selective separation of U(VI) over Mo(VI) using novel 2,9-diamide-1,10-phenanthroline ligands: Liquid-liquid extraction and coordination chemistry. Chin Chem Lett 34:108440. https://doi.org/10.1016/j.cclet.2023.108440
15. Liu F, Xiu TY, Shehzad H, Jin W, Huang ZW, Yang CC, Fu X, Wang XP, Shi WQ, Yuan LY (2024) Selective Separation of U(VI) from Pu(IV) by 2,9-Diamide-1,10-phenanthroline Ligands at High Acidity: Extraction and Coordination Chemistry. Inorg Chem 63:3859–3869. https://doi.org/10.1021/acs.inorgchem.3c04173
16. Yang Z, Chen G, Weng H, Shen W, Huang Z, Lin M (2018) Efficient and selective separation of U(VI) and Th(IV) from rare earths using functionalized hierarchically mesoporous silica. J Mater Sci 53:3398–3416. https://doi.org/10.1007/s10853-017-1808-9
17. Chen Y, Zhang P, Jiao L, Chen G, Yang Y, Chong H, Lin M (2022) High efficient and selective removal of U(VI) from lanthanides by phenanthroline diamide functionalized carbon doped boron nitride. Chem Eng J 446:137337. https://doi.org/10.1016/j.cej.2022.137337
18. Li F, Yang Z, Weng H, Chen G, Lin M, Zhao C (2018) High efficient separation of U(VI) and Th(IV) from rare earth elements in strong acidic solution by selective sorption on phenanthroline diamide functionalized graphene oxide. Chem Eng J 332:340–350. https://doi.org/10.1016/j.cej.2017.09.038
19. Simonin JP (2016) On the comparison of pseudo-first order and pseudo-second order rate laws in the modeling of adsorption kinetics. Chem Eng J 300:254–263. https://doi.org/10.1016/j.cej.2016.04.079
20. Ho YS, McKay G (1999) Pseudo-second order model for sorption processes. Process Biochem 34:451–465. https://doi.org/10.1016/S0032-9592(98)00112-5

Supplementary Files

This is a list of supplementary files associated with this preprint. Click to download.

- JRNCSupplementaryinformation.docx